Published in final edited form as:
*Science*. 2014 March 28; 343(6178): 1249288. doi:10.1126/science.1249288.

# Microbiota-Dependent Crosstalk Between Macrophages and ILC3 Promotes Intestinal Homeostasis

**Arthur Mortha**[1,2,3], **Aleksey Chudnovskiy**[1,2,3], **Daigo Hashimoto**[1,2,3,*], **Milena Bogunovic**[1,2,3,†], **Sean P. Spencer**[4], **Yasmine Belkaid**[4], and **Miriam Merad**[1,2,3,‡]

[1]Department of Oncological Sciences, 1470 Madison Avenue, New York, NY 10029, USA.

[2]The Tisch Cancer Institute, 1470 Madison Avenue, New York, NY 10029, USA.

[3]The Immunology Institute Mount Sinai School of Medicine, 1470 Madison Avenue, New York, NY 10029, USA.

[4]Program in Barrier Immunity and Repair, Mucosal Immunology Section, Laboratory of Parasitic Diseases, National Institute of Allergy and Infectious Diseases, Bethesda, MD 20892, USA.

## Abstract

The intestinal microbiota and tissue-resident myeloid cells promote immune responses that maintain intestinal homeostasis in the host. However, the cellular cues that translate microbial signals into intestinal homeostasis remain unclear. Here, we show that deficient granulocyte-macrophage colony-stimulating factor (GM-CSF) production altered mononuclear phagocyte effector functions and led to reduced regulatory T cell ($T_{reg}$) numbers and impaired oral tolerance. We observed that ROR$\gamma t^+$ innate lymphoid cells (ILCs) are the primary source of GM-CSF in the gut and that ILC-driven GM-CSF production was dependent on the ability of macrophages to sense microbial signals and produce interleukin-1β. Our findings reveal that commensal microbes promote a crosstalk between innate myeloid and lymphoid cells that leads to immune homeostasis in the intestine.

---

The gastrointestinal tract is colonized by an extraordinarily large number of commensal microbes and is constantly exposed to ingested antigens and potential pathogens. Regulation of intestinal tolerance thus represents the main task of the immune system of the gut mucosa. Defective immune tolerance in the gut is associated with the onset of inflammatory bowel diseases (IBD), a severe intestinal pathology that results from a dysregulated immune response to commensal microbes leading to chronic intestinal inflammation (1, 2).



‡Corresponding author. miriam.merad@mssm.edu.
*Present address: Department of Hematology, Hokkaido University Graduate School of Medicine, N15 W7, Kita-Ku, Sapporo 060-8638, Japan.
†Present address: Department of Microbiology and Immunology, Penn State College of Medicine and Milton S. Hershey Medical Center, 500 University Drive, Hershey, PA, USA.

**Supplementary Materials**
www.sciencemag.org/content/343/6178/1249288/suppl/DC1
Materials and Methods
Figs. S1 to S9
Reference (59, 60)

Accumulated evidence suggests that gut commensals contribute to the maintenance of intestinal homeostasis, partly through their ability to control the differentiation of effector T lymphocytes in the mucosa (3, 4) and to modulate inflammatory responses through the induction of $T_{regs}$ and interleukin-10 (IL-10) production (4–6).

Tissue-resident mononuclear phagocytes (MNPs) are equipped to detect a wide range of microbial signals and to capture and process extracellular antigens, including commensal microbial antigens in the form of peptide–major histocompatibility complexes (MHCs) that can be recognized by T lymphocytes (7). Mucosal tissue-resident MNPs consist of two main cell populations, macrophages (MPs) and dendritic cells (DCs) (8). Tissue-resident macrophages are characterized as $MHCII^+CD11c^+CD103^-CD11b^+CX3CRl^+F4/80^+CD64^+$ cells, whereas tissue-resident DCs are characterized as $MHCII^+CD11c^+CX3CR1^{int/-}F4/80^-CD64^-$ (fig. S1). DCs can further be subdivided into $CD103^+CD11b^-$ ($CD103^+$ DCs), $CD103^+CD11b^+$ (double-positive or DP DCs), $CD103^-CD11b^+$ ($CD11b^+$ DCs), and $CD103^-CD11b^+CD64^+F4/80^+$ (MP) subsets (9–12) (fig. S1). Both DCs and macrophages have been shown to contribute to the maintenance of intestinal immune tolerance through the induction or expansion of $T_{regs}$ in the intestine (13–19). Despite their key role in microbial sensing and immune tolerance, the cellular and molecular cues that translate microbial signals into immunoregulatory MNPs in the intestine remain poorly understood.

The cytokine granulocyte-macrophage colony-stimulating factor (GM-CSF), recently renamed colony-stimulating factor 2 (Csf2), is a key determinant of myeloid lineage differentiation and is required for the optimal function of tissue MNPs, including macrophages and DCs, thereby promoting host protection against environmental pathogens and vaccine responses (20, 21). Despite the key role of Csf2 in promoting MNP survival, differentiation, and function, previous studies reported that mice lacking Csf2 or its receptor displayed only minor impairment in the development of spleen and lymph node DCs (22). Subsequent studies showing that Csf2 expression is increased in inflamed mice and that adoptively transferred monocytes generate DCs in the inflamed spleen but not in the steady-state spleen suggested that Csf2 is a major proinflammatory cytokine that controls the differentiation of inflammatory but not steady-state DCs in vivo (23, 24). These results are consistent with the contribution of Csf2 to the pathophysiology of numerous inflammatory and autoimmune diseases (25–27).

In contrast, we recently observed that although Csf2-deficient mice have normal numbers of lymphoid tissue-resident DCs, they display a significant reduction in steady-state nonlymphoid tissue-resident DCs, including the $CD103^+CD11b^+$ DC subset found in the small intestine lamina propia (11,28), which have been implicated in the induction of lamina propria $T_{regs}$ (14, 15). These results prompted us to further explore the contribution of Csf2 to intestinal immune homeostasis in vivo.

## Regulation of Gut DC, Macrophage, and $T_{reg}$ Cell Homeostasis by Csf2

We characterized the mucosal T cell compartment in Csf2 -deficient mice ($Csf2^{-/-}$) in the steady state. Surprisingly, we observed a significant reduction in the frequency, number, and

proliferation of $CD45^+TCR\beta^+CD4^+Foxp3^+$ $T_{regs}$ in the colon of *Csf2*$^{-/-}$ mice compared to littermate controls (Fig. 1A and fig. S2A). The reduced $T_{reg}$ number was specific to the colon and was not observed in the small intestine of *Csf2*$^{-/-}$ mice. The reduction in the number of colonic $T_{regs}$ was associated with a significant reduction in the frequency and number of IL-10- and IL-2-producing T cells, along with a significant increase in the number of colonic interferon-γ (IFN-γ)-producing T cells, whereas IL-17-producing T cells were unaffected in 6-week-old *Csf2*$^{-/-}$ mice compared to wild-type mice (Fig. 1B and fig. S2B). Histological analysis of colonic sections from Csf2-deficient animals did not reveal overt inflammatory infiltrates in the lamina propria (fig. S2C).

Because Csf2 plays a critical role in the differentiation and function of tissue MNPs, we hypothesized that the alterations in T helper cell subsets observed in the colon of *Csf2*$^{-/-}$ animals might be due to defects in mucosal MNPs. Accordingly, we found reduced numbers of colonic DCs and macrophages in the absence of Csf2 (Fig. 1, C and D), thus establishing an important role for Csf2 in the homeostasis of the colonic MNP pool. DCs and macrophages have been reported to generate $Foxp3^+$ $T_{regs}$, via the production of the regulatory mediators retinoic acid (RA) and IL-10 in the presence of transforming growth factor-β (TGF-β). Thus, we analyzed the capacity of DCs and macrophages to produce these regulatory mediators in the absence of Csf2. We observed a significant reduction in the activity of the RA-generating enzyme retinaldehyde dehydrogenase (ALDH) throughout all colonic DC subsets and macrophages in *Csf2*$^{-/-}$ mice (Fig. 1E and fig. S2D) associated with reduced expression of *Aldh1* transcripts (fig. S2, E and F). Absence of Csf2 was also associated with a significant reduction in the release of TGF-β by colonic $CD103^+CD11b^+$ DCs and with reduced IL-10 secretion by macrophages (Fig. 1, F and G), which extends previous observations showing that Csf2 controls IL-10 and TGF-β release by peritoneal macrophages upon uptake of apoptotic cells (29). Notably, expression of *Aldh1a2* and *Il10*, and release of IL-10 were restored in *Csf2*$^{-/-}$ macrophages upon addition of exogenous Csf2 (fig. S2, G and H).

These findings suggest that the absence of Csf2 results in a reduction in the number, frequency, and function of DCs and macrophages in the colon. We thus sought to determine whether the alterations in T helper cell subsets observed in *Csf2*$^{-/-}$ animals was due to impaired MNP function. Accordingly, we found that colonic macrophages and DCs isolated from *Csf2*$^{-/-}$ mice were compromised in their ability to drive $T_{reg}$ differentiation ex vivo compared to their *Csf2*$^{+/+}$ counterparts (Fig. 1H). This was reversed upon addition of exogenous Csf2 (Fig. 1H), suggesting that the reduced $T_{reg}$ pool observed in *Csf2*$^{-/-}$ mice was a consequence of impaired mucosal MNP function and not only reduced MNP numbers. Critically, administration of B16 melanoma cells that overexpressed Csf2 to *Csf2*$^{-/-}$ mice restored MNP numbers (fig. S3A) and increased $T_{reg}$ frequency (Fig. 1I), while reducing the number of IFNγ-producing intestinal T cells to levels comparable to those of untreated C57Bl/6 mice (fig. S3B), consistent with the ability of exogenous Csf2 to restore the immunoregulatory potential of *Csf2*$^{-/-}$ macrophages and DCs ex vivo (Fig. 1H). Together, these data establish Csf2 as a master regulator of MNP immunoregulatory function in the steady-state colon tissue.

Notably, blockade of RA production [with 4-diethly-aminobenzaldehyde (DEAB)] and/or blockade of IL-10 [with monoclonal antibody (mAb) against IL-10] abrogated the ability of Csf2 to rescue $T_{reg}$ induction in vitro by *Csf2*$^{-/-}$ MNPs, whereas addition of RA rescued $T_{reg}$ induction in these cultures (fig. S3, C and D). Consistent with these findings, injection of the RA receptor antagonist LE540 compromised Csf2-mediated rescue of $T_{regs}$ in *Csf2*$^{-/-}$ mice in vivo (fig. S3E), and conversely, injection of RA but not IL-10 restored $T_{reg}$ frequency in *Csf2*$^{-/-}$ mice in vivo (fig. S3F).

## Csf2 Is Produced by RORγt$^{+}$ ILC3

Our results showing that colonic $T_{reg}$ homeostasis was dependent on Csf2 prompted us to characterize the source of Csf2 in a noninflamed intestine. Previous reports have suggested that Csf2 is primarily produced by radio-resistant epithelial cells (30), including Paneth cells (31) in the gut. Surprisingly, we found that in the large and small intestine, Csf2 was constitutively produced by tissue-resident CD45$^{+}$ hematopoietic cells expressing the retinoic acid–related orphan receptor γ t (RORγt) (Fig. 2A). RORγt$^{+}$ T helper 17 ($T_H17$) cells can produce large amounts of Csf2 in the inflamed brain and intestine (26, 27, 32). Other RORγt-dependent cell populations include group 3 innate lymphoid cells (ILC3) composed of lymphoid tissue–inducer (LTi) cells and RORγt$^{+}$ ILC expressing the natural killer (NK) cell receptor, NKp46, recently termed NCR$^{+}$ILC3 cells (33).

LTi cells and NCR$^{+}$ILC3 are highly abundant in the small and large intestine in the steady state (34). To test whether RORγt$^{+}$ ILC3 contribute to the steady-state production of Csf2 in the intestine, we measured Csf2 production in *Rorc*$^{-/-}$mice, which lack RORγt-expressing cells (35). Csf2 expression was reduced in the large and small intestine of *Rorc*$^{-/-}$ mice and declined to levels almost as low as those found in *Csf2*$^{-/-}$animals (Fig. 2B), suggesting that steady-state production of the Csf2 cytokine in the intestine was predominantly mediated by RORγt$^{+}$ cells. Accordingly, we observed that 80% of Csf2-producing cells in the normal small and large intestine resided within the CD3$^{-}$CD45$^{+}$RORγt$^{+}$ compartment, consistent with the phenotype of RORγt$^{+}$ ILC3 (Fig. 2, A and C). Csf2 was produced by both subsets of RORγt$^{+}$ ILC3, including LTi cells and NCR$^{+}$ ILC3, in the small and large intestine but not by NKp46$^{+}$RORγt$^{-}$ NK cells (33) (Fig. 2D). These results are consistent with previous data showing that human RORγt-expressing NKp44$^{+}$ ILC produce Csf2 (36). RORγt$^{+}$ ILC3 are reportedly localized within the isolated lymphoid follicles (ILFs) (37, 38), so we used *Rorc*$^{+/EGFP}$ reporter animals to confirm that Csf2$^{+}$ cells are enriched in ILF throughout the lamina propria (Fig. 2E and fig. S4, A to E). Areas enriched in RORγt$^{+}$ cells (ILFs) also contained significantly higher levels of Csf2 transcripts when compared with intestinal epithelial cells, Peyer's patches, and lamina propria depleted of ILF (Fig. 2, F and G, and fig. S4, A to E). These data identify RORγt$^{+}$ ILC3 in ILFs as the main producers of intestinal Csf2 in the steady state.

Analysis of bone marrow chimeric mice that were lethally irradiated and then reconstituted with congenic hematopoietic progenitors revealed that host-derived RORγt$^{+}$ ILC3 remained resident in the recipient intestine for several months after lethal body irradiation, consistent with previously published data (39). We observed high levels of Csf2 production in host-derived RORγt$^{+}$ ILC3 even 3 months after lethal body irradiation (fig. S5), suggesting that

RORγt$^+$ ILC3 likely contribute to the steady-state radio-resistant source of Csf2 reported by other investigators (30). Fluorescence-activated cell sorting (FACS) purification of ILC subsets from *Rorc*$^{+/EGFP}$ reporter animals further confirmed RORγt$^+$ ILC3 as major producers of Csf2 (Fig. 2H). Accordingly, although Csf2-producing cells were detectable in high numbers in the small and large intestine of *Rag2*$^{-/-}$ mice, which lack RORγt-expressing T lymphocytes but not ILCs (Fig. 2I), they were reduced in ILC-deficient *Rag2*$^{-/-}$*Il2rg*$^{-/-}$ mice and in *Rag2*$^{-/-}$ mice depleted of ILCs with mAb against CD90 (34) (Fig. 2J). ILC depletion in *Rag2*$^{-/-}$ mice led to impaired RA-generating enzyme activity in colonic DCs and macrophages (fig. S6). Together, these results establish ILCs as a key producer of the myeloid regulatory cytokine Csf2 in the intestine.

## Csf2 Production Is Dependent on Microbial Signals

The effector functions of RORγt$^+$ ILC3, and the development and maturation of ILFs depend on commensal-driven signals (37, 40, 41). We found that Csf2 production was absent in newborns, slightly increased in 7-day-old mice, and increased substantially from day 14 after birth, concurrent with the increase in numbers and complexity of the intestinal microbial flora at these developmental stages (Fig. 3, A and B). To further investigate the influence of the commensal flora on Csf2 production in the intestine, we treated adult mice with broad-spectrum antibiotics known to strongly reduce the gut microbiota. In accordance with our findings in newborn animals, adult mice treated with broad-spectrum antibiotics displayed reduced Csf2 production in the small and large intestine (Fig. 3C). These results suggest that commensal-driven signals control the steady-state production of Csf2 by RORγt$^+$ ILC3 in the mouse intestine.

Murine RORγt$^+$ ILC3 lack Toll-like receptors (TLRs) and cannot directly sense microbial signals in the gut; hence, these cells must rely on other cellular sensors to translate cues from commensal bacteria into effector functions (42). We therefore explored whether cytokines derived from myeloid cells could drive Csf2 production by RORγt$^+$ ILC3 ex vivo. Among several cytokines tested, we observed that IL-1β was a particularly potent inducer of Csf2 production by RORγt$^+$ ILC3 (Fig. 3C), consistent with the reported role of IL-1β as a potent driver of ILC function (38). Because the myeloid cytokine IL-23 promotes the production of the cytokine IL-22 by RORγt$^+$ ILC3, we examined whether IL-23 also promoted Csf2 production by these cells (43). IL-23 was unable to promote Csf2 production by RORγt$^+$ ILC3 (fig. S7A), whereas it stimulated the release of IL-22 (fig. S7B), as previously reported (43). Furthermore, IL-22 production by RORγt$^+$ ILC3 was unaffected in *Csf2*$^{-/-}$ mice (fig. S7C). Exposure to IL-1β rescued Csf2 production by RORγt$^+$ ILC3 isolated from antibiotic-treated mice (Fig. 3C). Accordingly, LTi and NCR$^+$ ILC3 isolated from mice lacking IL-1 receptor 1 (*Il1r1*$^{-/-}$) failed to produce Csf2 (Fig. 3D), thereby implicating IL-1β and IL-1R signaling as key drivers of Csf2 production in the intestine. In contrast, absence of the other IL-1 superfamily member, IL-18, did not compromise intestinal Csf2 production (fig. S7D). Together, these data indicate that IL-1β–producing cells that respond to microbial signals control the steady-state production of Csf2 by RORγt$^+$ ILC3 in the intestine.

Sensing the commensal microflora by the TLR and the activation of the adapter protein Myd88 is critical for maintaining intestinal homeostasis (44) and leads to steady-state IL-1β

production by tissue MNPs (45). Tissue-resident macrophages, $CD103^+$ DCs, and $CD103^-$ DCs arise from different developmental pathways and express distinct pattern recognition receptors (46). We found that intestinal macrophages were the highest producers of *Il1b* and IL-1β protein, as previously reported (45, 47), suggesting that this population is a key regulator of Csf2 production in the gut (Fig. 3, E and F).

Because microbial signals were required to drive Csf2 production in the intestine, we next examined whether deletion of the TLR-adapter protein Myd88 in phagocytes influenced Csf2 production by RORγt$^+$ ILC3. Lysozyme M (LysM) is expressed at high levels in macrophages relative to DCs (48), and notably, mice that lack Myd88 specifically in LysM$^+$ cells [$LysM^{Cre}$ $xMyd88^{flox/flox}$ ($Myd88^{\Delta MP}$) mice] exhibited a significant reduction in IL-1β production in intestinal macrophages, whereas IL-1β production by intestinal DCs was unaffected (Fig. 3F). The disruption of IL-1b release by intestinal macrophages in $Myd88^{\Delta MP}$ mice abrogated the production of Csf2 by RORγt$^+$ LTi and NCR$^+$ ILC3 in these animals (Fig. 3G), whereas addition of exogenous IL-1β cytokine rescued Csf2 production by RORγt$^+$ ILC3 (Fig. 3G). Consistent with a central role for macrophages in intestinal IL-1β production, administration of depleting anti-Csf1 receptor monoclonal antibody (anti-Csf1R mAb) depleted tissue macrophages (Fig. 3H), as we previously showed (49), and reduced total *Il1b* expression (Fig. 3I). Accordingly, Csf2 production by intestinal RORγt$^+$ ILC3 was significantly reduced after depletion of colonic macrophages (Fig. 3J). IL-1β cytokine was capable of rescuing Csf2 production by RORγt$^+$ ILC3 isolated from mice treated with the anti-Csf1R mAb (Fig. 3J), thus confirming that macrophage-derived IL-1β is a key driver of Csf2 production by RORγt$^+$ ILC3. Myd88 is an essential signal transducer in both the TLR and IL-1R pathway (50). To establish whether IL-1β and IL-1R signaling are required to promote Csf2 production by RORγt$^+$ ILC3, we crossed $Rorc^{Cre}$ mice with $Myd88^{flox/flox}$ mice to achieve deletion of Myd88 specifically in RORγt$^+$ ILC3 and T cells ($Myd88^{\Delta T/LTi}$ ) (51). As expected, we observed a reduction in Csf2 production by RORγt$^+$ ILC3 from $Myd88^{\Delta T/LTi}$ mice (Fig. 3K). In this case, administration of IL-1β cytokine failed to rescue Csf2 expression by RORγt$^+$ ILC3, suggesting that Myd88 functions downstream of IL-1R in RORγt$^+$ ILC3 (Fig. 3K). Taken together, our results suggest that Myd88-dependent sensing of the commensal microflora by intestinal macrophages elicits production of IL-1β, which in turn activates the IL-1R–Myd88 pathway in RORγt$^+$ ILC3 to drive the steady-state production of Csf2. Alteration of the commensal flora using broad-spectrum antibiotics or deletion of macrophages using anti-Csf1R mAb treatment led to impaired RA production in all DC subsets (fig. S8A) and to reduced $T_{reg}$ numbers and proliferation (fig. S8, B and C), confirming the role of tissue macrophages in translating microbial cues into immunoregulatory signals that help promote $T_{reg}$ homeostasis in the steady-state colon.

## Csf2 Promotes Oral Tolerance to Fed Antigens

Because one of the key functions of intestinal $T_{regs}$ is the maintenance of oral tolerance to fed antigens, we asked whether deficiency in Csf2 affects de novo generation of intestinal $T_{regs}$ upon oral administration of ovalbumin (OVA). Conversion and expansion of OVA-specific $T_{regs}$ in the small and large intestine were impaired in $Csf2^{-/-}$mice compared to wild-type mice (Fig. 4, A and B). Similar results were obtained when $T_{reg}$ conversion was analyzed in mice selectively lacking Csf2 in RORγt$^+$ ILC3 ($Myd88^{\Delta T/LTi}$) or in ILC-

deficient mice (*Rag2*$^{-/-}$*Il2rg*$^{-/-}$) (Fig. 4, C and D). Consistent with Csf2's key role in oral tolerance, OVA feeding of *Csf2*$^{-/-}$ mice and *Myd88*$^{\Delta T/LTi}$ mice failed to protect the mice from delayed-type hypersensitivity (DTH) reaction upon OVA challenge, whereas control mice were protected (Fig. 4E). Together, these results establish that altered Csf2 production by ILCs impairs the induction of oral tolerance to dietary antigens. The defect in $T_{reg}$ conversion observed in the small intestine of *Csf2*$^{-/-}$ mice contrasts with the apparent normal total $T_{reg}$ numbers observed in the small bowel of these mice. These results suggest that compensatory mechanisms specific to the small bowel may help restore the number but likely not the repertoire of small intestinal $T_{regs}$ in *Csf2*$^{-/-}$ mice.

To establish the direct contribution of Csf2 produced by ILC3 to $T_{reg}$ conversion in vivo, we reconstituted ILC-deficient *Rag2*$^{-/-}$*Il2rg*$^{-/-}$ mice with *Csf2*$^{-/-}$ or *Csf2*$^{+/+}$ ILC3. Two weeks later, *Rag2*$^{-/-}$*Il2rg*$^{-/-}$ mice reconstituted with ILCs were adoptively transferred with OVA-specific T cell receptor transgenic OTII cells and fed with OVA for 5 days. *Csf2*$^{-/-}$ and *Csf2*$^{+/+}$ ILC3 engrafted with the same efficiency in *Rag2*$^{-/-}$*Il2rg*$^{-/-}$ mice (Fig. 4F), and reconstitution of *Rag2*$^{-/-}$*Il2rg*$^{-/-}$ mice with *Csf2*$^{+/+}$ ILC3 led to partial recovery of Csf2 production in the intestine (Fig. 4F). Although the rate of $T_{reg}$ conversion was low in all *Rag2*$^{-/-}$*Il2rg*$^{-/-}$mice due to a defect in lymphoid organ development in these mice, OVA-specific $T_{reg}$ conversion was nonetheless significantly higher in *Rag2*$^{-/-}$*Il2rg*$^{-/-}$mice reconstituted with *Csf2*$^{+/+}$ compared to mice reconstituted with *Csf2*$^{-/-}$ ILC3 (Fig. 4G), further emphasizing the contribution of ILC3-derived Csf2 to the control of oral tolerance to dietary antigens.

## Discussion

Previous studies have established the role of microbial commensals that colonize the large bowel to promote the induction of Foxp3$^{+}$ $T_{reg}$ differentiation (5). However the cellular cues that promote $T_{reg}$ accumulation in response to gut commensals have only recently started to be unraveled (52–54). Our data identify a mechanism by which the gut microbiota promotes intestinal homeostasis by supporting a crosstalk between IL-1β–secreting macrophages and Csf2-producing RORγt$^{+}$ ILC3 in the intestinal mucosa. Microbiota-driven IL-1b production by macrophages promoted the release of Csf2 by ILC3, which in turn acted on DCs and macrophages, allowing for the maintenance of colonic $T_{reg}$ homeostasis (fig. S9). Ablation of Csf2 altered DC and macrophage numbers and impaired their ability to produce regulatory factors such as RA and IL-10, which led to disrupted $T_{reg}$ homeostasis in the large intestine. Conversely, administration of Csf2 cytokine increased $T_{reg}$ frequency in the gut. Most notably, cell type– specific ablation of IL-1–dependent signaling in RORγt$^{+}$ ILC3 abrogated oral tolerance to dietary antigens and compromised intestinal $T_{reg}$ homeostasis in vivo. Although the reduction in total $T_{reg}$ numbers was mostly observed in the large intestine, adoptive transfer studies in *Csf2*$^{-/-}$ mice revealed impaired $T_{reg}$ differentiation both in the small and large intestine, suggesting that Csf2-dependent MNP immunoregulatory functions control $T_{reg}$ induction in both tissues

Establishing intestinal tolerance is critical for the prevention of intestinal diseases such as IBD. IBD includes two broad disease classifications known as ulcerative colitis and Crohn's disease, but there is substantial variation in IBD clinicopathology in individual patients;

hence, it is likely that numerous subtypes of IBD exist in this group. In a study of more than 300 patients with Crohn's disease, the presence of neutralizing antibodies to Csf2 in the serum correlated with ileal involvement and the development of penetrating pathology, whereas a more recent study identified reduced levels of Csf2 receptor (Csf2R) and impaired receptor activity in a mixed group of IBD patients (55, 56). Previous clinical trials of recombinant Csf2 in IBD have established patient benefit in terms of reduced disease severity and lower burden of corticosteroid use (57). Unpublished results of a larger trial of Csf2 in IBD has since failed to achieve primary clinical end points, but it remains likely that a subset of IBD patients with defective Csf2 production or function could benefit from this therapy.

The uncovered key role for Csf2 in the maintenance of intestinal tolerance is consistent with previous studies showing that absence of Csf2 can also contribute to lupus-like disease, insulitis, and age-related glucose intolerance (29, 58) and further emphasizes the critical role of tissue-resident phagocytes in the maintenance of tissue integrity.

Our data reveal a mechanism by which the gut commensal flora promotes immune homeostasis in the host. We have identified the commensal-driven MNP-ILC-Csf2 axis as a key regulator of intestinal T cell homeostasis in the mouse intestine. Disturbance of this axis radically altered MNP effector function, resulting in impaired oral tolerance to dietary antigens. These results represent an important advance in our understanding of how commensal microbes can regulate host intestinal immunity and may inform the design of new immunotherapies for the use in patients with subtypes of IBD.

## Supplementary Material

Refer to Web version on PubMed Central for supplementary material.

## Acknowledgments

We thank the Merad laboratory for helpful discussions and input. We are grateful to W.-H. Kwan and W. van der Touw for assistance with the $T_{reg}$ induction assay. We thank R. Huq and L. O'Rourke at the Icahn School of Medicine at Mount Sinai Microscopy Shared Resource Facility for their training, helpful advice, and support with microscopy imaging. We are grateful to C. Berin and A. Belén Blázquez for support with the oral tolerance and DTH models. We thank J. Ochando and the Flow Cytometry facility for technical support and assistance with cell sorting. The data presented in this paper are tabulated in the main paper and in the supporting materials. M.M. is funded by NIH grants R01 CA154947A, R01 CA173861, and U01 AI095611. A.M. is funded by the German Research Foundation (DFG) grant MO2380/1-1. Y.B. was supported by the Division of Intramural Research of the National Institute of Allergy and Infectious Diseases.

## References and Notes

1. Maloy KJ, Powrie F. Intestinal homeostasis and its breakdown in inflammatory bowel disease. Nature. 2011; 474:298–306. pmid: 21677746. [PubMed: 21677746]
2. Khor B, Gardet A, Xavier RJ. Genetics and pathogenesis of inflammatory bowel disease. Nature. 2011; 474:307–317. pmid: 21677747. [PubMed: 21677747]
3. Ivanov II, et al. Induction of intestinal Th17 cells by segmented filamentous bacteria. Cell. 2009; 139:485–498. pmid: 19836068. [PubMed: 19836068]
4. Hooper LV, Littman DR, Macpherson AJ. Interactions between the microbiota and the immune system. Science. 2012; 336:1268–1273. pmid: 22674334. [PubMed: 22674334]

5. Atarashi K, et al. Induction of colonic regulatory T cells by indigenous Clostridium species. Science. 2011; 331:337–341. pmid: 21205640. [PubMed: 21205640]
6. Round JL, et al. The Toll-like receptor 2 pathway establishes colonization by a commensal of the human microbiota. Science. 2011; 332:974–977. pmid: 21512004. [PubMed: 21512004]
7. Merad M, Sathe P, Helft J, Miller J, Mortha A. The dendritic cell lineage: Ontogeny and function of dendritic cells and their subsets in the steady state and the inflamed setting. Annu. Rev. Immunol. 2013; 31:563–604. pmid: 23516985. [PubMed: 23516985]
8. Bogunovic M, Mortha A, Muller PA, Merad M. Mononuclear phagocyte diversity in the intestine. Immunol. Res. 2012; 54:37–49. pmid: 22562804. [PubMed: 22562804]
9. Cerovic V, et al. Intestinal CD103(-) dendritic cells migrate in lymph and prime effector T cells. Mucosal Immunol. 2013; 6:104–113. pmid: 22718260. [PubMed: 22718260]
10. Tamoutounour S, et al. CD64 distinguishes macrophages from dendritic cells in the gut and reveals the Th1-inducing role of mesenteric lymph node macrophages during colitis. Eur. J. Immunol. 2012; 42:3150–3166. pmid: 22936024. [PubMed: 22936024]
11. Bogunovic M, et al. Origin of the lamina propria dendritic cell network. Immunity. 2009; 31:513–525. pmid: 19733489. [PubMed: 19733489]
12. Varol C, et al. Intestinal lamina propria dendritic cell subsets have different origin and functions. Immunity. 2009; 31:502–512. pmid: 19733097. [PubMed: 19733097]
13. Takeda K, et al. Enhanced Th1 activity and development of chronic enterocolitis in mice devoid of Stat3 in macrophages and neutrophils. Immunity. 1999; 10:39–49. pmid: 10023769. [PubMed: 10023769]
14. Sun CM, et al. Small intestine lamina propria dendritic cells promote de novo generation of Foxp3 T reg cells via retinoic acid. J. Exp. Med. 2007; 204:1775–1785. pmid: 17620362. [PubMed: 17620362]
15. Coombes JL, et al. A functionally specialized population of mucosal CD103+ DCs induces Foxp3+ regulatory T cells via a TGF-beta and retinoic acid-dependent mechanism. J. Exp. Med. 2007; 204:1757–1764. pmid: 17620361. [PubMed: 17620361]
16. Denning TL, Wang YC, Patel SR, Williams IR, Pulendran B. Lamina propria macrophages and dendritic cells differentially induce regulatory and interleukin 17-producing T cell responses. Nat. Immunol. 2007; 8:1086–1094. pmid: 17873879. [PubMed: 17873879]
17. Manicassamy S, et al. Activation of beta-catenin in dendritic cells regulates immunity versus tolerance in the intestine. Science. 2010; 329:849–853. pmid: 20705860. [PubMed: 20705860]
18. Hadis U, et al. Intestinal tolerance requires gut homing and expansion of FoxP3+ regulatory T cells in the lamina propria. Immunity. 2011; 34:237–246. pmid: 21333554. [PubMed: 21333554]
19. Denning TL, et al. Functional specializations of intestinal dendritic cell and macrophage subsets that control Th17 and regulatory T cell responses are dependent on the T cell/APC ratio, source of mouse strain, and regional localization. J. Immunol. 2011; 187:733–747. pmid: 21666057. [PubMed: 21666057]
20. Jinushi M, Hodi FS, Dranoff G. Enhancing the clinical activity of granulocyte-macrophage colony-stimulating factor-secreting tumor cell vaccines. Immunol. Rev. 2008; 222:287–298. pmid: 18364009. [PubMed: 18364009]
21. Zhan Y, Xu Y, Lew AM. The regulation of the development and function of dendritic cell subsets by GM-CSF: More than a hematopoietic growth factor. Mol. Immunol. 2012; 52:30–37. pmid: 22580403. [PubMed: 22580403]
22. Vremec D, et al. The influence of granulocyte/macrophage colony-stimulating factor on dendritic cell levels in mouse lymphoid organs. Eur. J. Immunol. 1997; 27:40–44. pmid: 9021996. [PubMed: 9021996]
23. Naik SH, et al. Intrasplenic steady-state dendritic cell precursors that are distinct from monocytes. Nat. Immunol. 2006; 7:663–671. pmid: 16680143. [PubMed: 16680143]
24. Shortman K, Naik SH. Steady-state and inflammatory dendritic-cell development. Nat. Rev. Immunol. 2007; 7:19–30. pmid: 17170756. [PubMed: 17170756]
25. Hamilton JA. Colony-stimulating factors in inflammation and autoimmunity. Nat. Rev. Immunol. 2008; 8:533–544. pmid: 18551128. [PubMed: 18551128]

26. Codarri L, et al. RORγt drives production of the cytokine GM-CSF in helper T cells, which is essential for the effector phase of autoimmune neuroinflammation. Nat. Immunol. 2011; 12:560–567. pmid: 21516112. [PubMed: 21516112]
27. El-Behi M, et al. The encephalitogenicity of T(H)17 cells is dependent on IL-1- and IL-23-induced production of the cytokine GM-CSF. Nat. Immunol. 2011; 12:568–575. pmid: 21516111. [PubMed: 21516111]
28. Greter M, et al. GM-CSF controls nonlymphoid tissue dendritic cell homeostasis but is dispensable for the differentiation of inflammatory dendritic cells. Immunity. 2012; 36:1031–1046. pmid: 22749353. [PubMed: 22749353]
29. Jinushi M, et al. MFG-E8-mediated uptake of apoptotic cells by APCs links the pro- and antiinflammatory activities of GM-CSF. J. Clin. Invest. 2007; 117:1902–1913. pmid: 17557120. [PubMed: 17557120]
30. Egea L, et al. GM-CSF produced by nonhematopoietic cells is required for early epithelial cell proliferation and repair of injured colonic mucosa. J. Immunol. 2013; 190:1702–1713. pmid: 23325885. [PubMed: 23325885]
31. Fukuzawa H, et al. Identification of GM-CSF in Paneth cells using single-cell RT-PCR. Biochem. Biophys. Res. Commun. 2003; 312:897–902. pmid: 14651956. [PubMed: 14651956]
32. Griseri T, McKenzie BS, Schiering C, Powrie F. Dysregulated hematopoietic stem and progenitor cell activity promotes interleukin-23-driven chronic intestinal inflammation. Immunity. 2012; 37:1116–1129. pmid: 23200826. [PubMed: 23200826]
33. Spits H, et al. Innate lymphoid cells—a proposal for uniform nomenclature. Nat. Rev. Immunol. 2013; 13:145–149. pmid: 23348417. [PubMed: 23348417]
34. Vonarbourg C, et al. Regulated expression of nuclear receptor RORγt confers distinct functional fates to NK cell receptor-expressing RORγt(+) innate lymphocytes. Immunity. 2010; 33:736–751. pmid: 21093318. [PubMed: 21093318]
35. Eberl G, et al. An essential function for the nuclear receptor RORgamma(t) in the generation of fetal lymphoid tissue inducer cells. Nat. Immunol. 2004; 5:64–73. pmid: 14691482. [PubMed: 14691482]
36. Cella M, et al. A human natural killer cell subset provides an innate source of IL-22 for mucosal immunity. Nature. 2009; 457:722–725. pmid: 18978771. [PubMed: 18978771]
37. Sanos SL, et al. RORgammat and commensal microflora are required for the differentiation of mucosal interleukin 22-producing NKp46+ cells. Nat. Immunol. 2009; 10:83–91. pmid: 19029903. [PubMed: 19029903]
38. Reynders A, et al. Identity, regulation and in vivo function of gut NKp46$^{+}$RORγt$^{+}$ and NKp46$^{+}$RORγt$^{-}$lymphoid cells. EMBO J. 2011; 30:2934–2947. pmid: 21685873. [PubMed: 21685873]
39. Hanash AM, et al. Interleukin-22 protects intestinal stem cells from immune-mediated tissue damage and regulates sensitivity to graft versus host disease. Immunity. 2012; 37:339–350. pmid: 22921121. [PubMed: 22921121]
40. Bouskra D, et al. Lymphoid tissue genesis induced by commensals through NOD1 regulates intestinal homeostasis. Nature. 2008; 456:507–510. pmid: 18987631. [PubMed: 18987631]
41. Satoh-Takayama N, et al. Microbial flora drives interleukin 22 production in intestinal NKp46+ cells that provide innate mucosal immune defense. Immunity. 2008; 29:958–970. pmid: 19084435. [PubMed: 19084435]
42. Crellin NK, et al. Regulation of cytokine secretion in human CD127(+) LTi-like innate lymphoid cells by Toll-like receptor 2. Immunity. 2010; 33:752–764. pmid: 21055975. [PubMed: 21055975]
43. Takatori H, et al. Lymphoid tissue inducer-like cells are an innate source of IL-17 and IL-22. J. Exp. Med. 2009; 206:35–41. pmid: 19114665. [PubMed: 19114665]
44. Rakoff-Nahoum S, Paglino J, Eslami-Varzaneh F, Edberg S, Medzhitov R. Recognition of commensal microflora by toll-like receptors is required for intestinal homeostasis. Cell. 2004; 118:229–241. pmid: 15260992. [PubMed: 15260992]
45. Shaw MH, Kamada N, Kim YG, Núñez G. Microbiota-induced IL-1β, but not IL-6, is critical for the development of steady-state TH17 cells in the intestine. J. Exp. Med. 2012; 209:251–258. pmid: 22291094. [PubMed: 22291094]

46. Hashimoto D, Miller J, Merad M. Dendritic cell and macrophage heterogeneity in vivo. Immunity. 2011; 35:323–335. pmid: 21943488. [PubMed: 21943488]
47. Hoshi N, et al. MyD88 signalling in colonic mononuclear phagocytes drives colitis in IL-10-deficient mice. Nat. Commun. 2012; 3:1120. pmid: 23047678. [PubMed: 23047678]
48. Jakubzick C, et al. Lymph-migrating, tissue-derived dendritic cells are minor constituents within steady-state lymph nodes. J. Exp. Med. 2008; 205:2839–2850. pmid: 18981237. [PubMed: 18981237]
49. Hashimoto D, et al. Pretransplant CSF-1 therapy expands recipient macrophages and ameliorates GVHD after allogeneic hematopoietic cell transplantation. J. Exp. Med. 2011; 208:1069–1082. pmid: 21536742. [PubMed: 21536742]
50. O'Neill LA, Bowie AG. The family of five: TIR-domain-containing adaptors in Toll-like receptor signalling. Nat. Rev. Immunol. 2007; 7:353–364. pmid: 17457343. [PubMed: 17457343]
51. Eberl G, Littman DR. Thymic origin of intestinal alphabeta T cells revealed by fate mapping of RORgammat+ cells. Science. 2004; 305:248–251. pmid: 15247480. [PubMed: 15247480]
52. Smith PM, et al. The microbial metabolites, short-chain fatty acids, regulate colonic Treg cell homeostasis. Science. 2013; 341:569–573. pmid: 23828891. [PubMed: 23828891]
53. Arpaia N, et al. Metabolites produced by commensal bacteria promote peripheral regulatory T-cell generation. Nature. 2013; 504:451–455. pmid: 24226773. [PubMed: 24226773]
54. Furusawa Y, et al. Commensal microbe-derived butyrate induces the differentiation of colonic regulatory T cells. Nature. 2013; 504:446–450. pmid: 24226770. [PubMed: 24226770]
55. Han X, et al. Granulocyte-macrophage colony-stimulating factor autoantibodies in murine ileitis and progressive ileal Crohn's disease. Gastroenterology. 2009; 136:1261–1271. e1-e3. pmid: 19230854. [PubMed: 19230854]
56. Goldstein JI, et al. Defective leukocyte GM-CSF receptor (CD116) expression and function in inflammatory bowel disease. Gastroenterology. 2011; 141:208–216. pmid: 21557945. [PubMed: 21557945]
57. Korzenik JR, Dieckgraefe BK, Valentine JF, Hausman DF, Gilbert MJ. Sargramostim in Crohn's Disease Study Group, Sargramostim for active Crohn's disease. N. Engl. J. Med. 2005; 352:2193–2201. pmid: 15917384. [PubMed: 15917384]
58. Enzler T, et al. Functional deficiencies of granulocyte-macrophage colony stimulating factor and interleukin-3 contribute to insulitis and destruction of beta cells. Blood. 2007; 110:954–961. pmid: 17483299. [PubMed: 17483299]

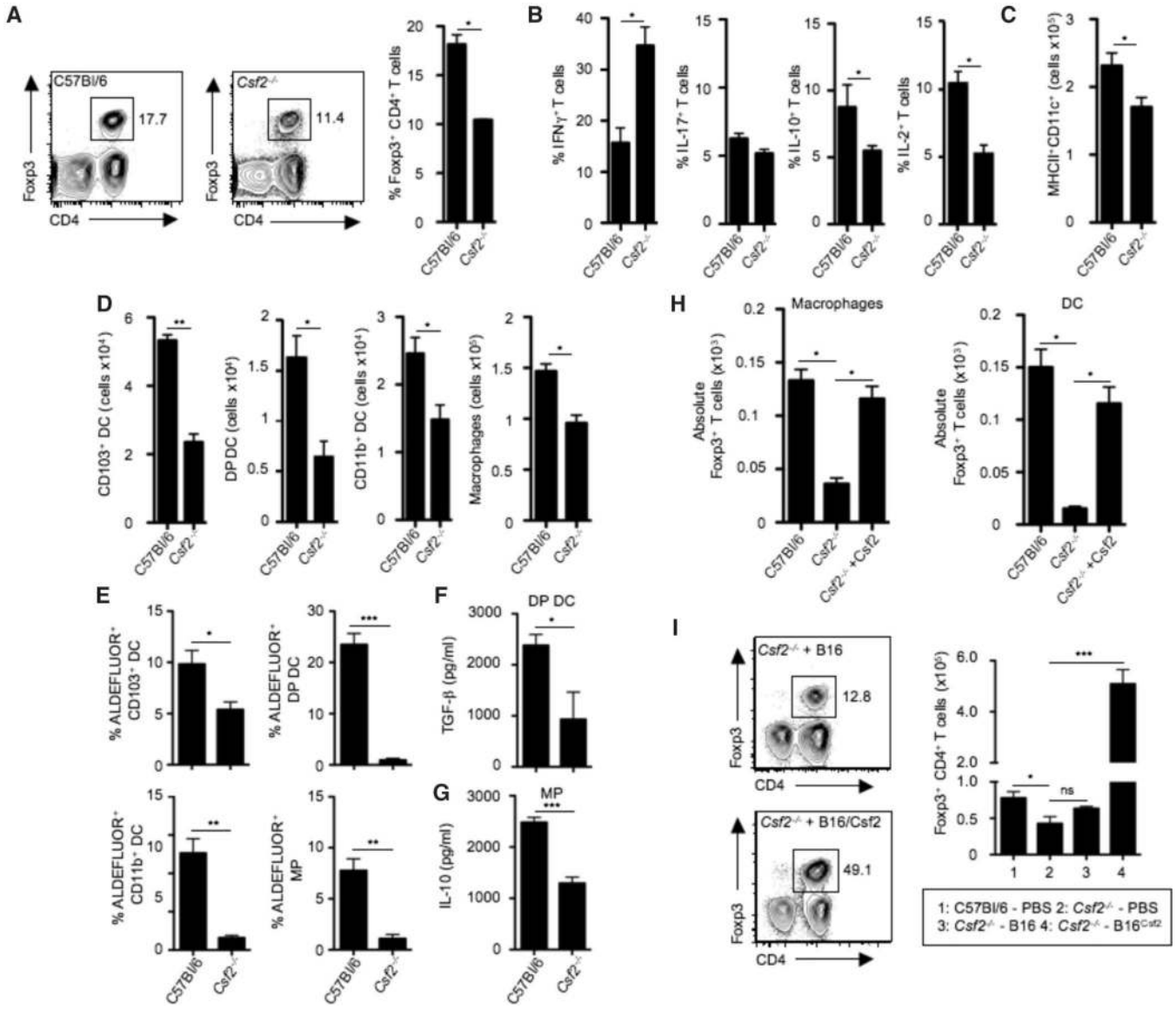


**Fig. 1. Csf2 regulates tissue mononuclear phagocyte frequency and effector functions required for T helper cell homeostasis**

(**A**) Contour plots and bar graph show percentages of $CD3^+CD4^+Foxp3^+$ colonic $T_{regs}$ among total colonic lamina propria $CD45^+$ cells in C57Bl/6 and *Csf2*$^{-/-}$ mice. (**B**) Bar graphs show percentages of $CD3^+CD4^+$ T cells producing IFN-γ, IL-17, IL-10, or IL-2 among total colonic $CD45^+$ cells in C57Bl/6 and *Csf2*$^{-/-}$ mice after 4 hours of stimulation with phorbol 12-myristate 13-acetate (PMA)–ionomycin in the presence of Brefeldin A. (**C**) Bar graphs show absolute numbers of $MHCII^+CD11c^+$ cells among total colonic $CD45^+$ cells in C57Bl/6 and *Csf2*$^{-/-}$ mice. (**D**) DCs were characterized as $CD45^+MHCII^+CD11c^+$ and further subdivided into $CD103^+$ DCs, $CD103^+CD11b^+$ DCs [double positive (DP) DCs], and $CD11b^+$ DCs. Macrophages (MP) were characterized as $MHCII^+CD11c^+CD11b^+F4/80^+CD64^+$ cells. Bar graphs show absolute numbers of $CD103^+$ DCs, DP DCs, $CD11b^+$ DCs, and MPs in C57Bl/6 and *Csf2*$^{-/-}$ mice. (**E**) Percentages of $ALDEFLUOR^+$ cells among each colonic DC subset and MPs in C57Bl/6 and *Csf2*$^{-/-}$ mice.

(**F** and **G**) Bar graphs show enzyme-linked immunosorbent assay (ELISA) measurement of TGF-β production by sorted DP DCs (F) and IL-10 production by sorted MPs (G). (**H**) Colonic MPs or DCs were FACS-sorted from C57Bl/6 or *Csf2*$^{-/-}$ mice and cocultured with naïve T cells alone or in the presence of exogenous Csf2. Bar graphs show absolute numbers of Foxp3$^{+}$ $T_{regs}$. Data are representative of six independent experiments and are shown as mean ± SD. (**I**) Contour plots show percentages of CD45$^{+}$CD3$^{+}$CD4$^{+}$Foxp3$^{+}$ colonic $T_{regs}$ in *Csf2*$^{-/-}$ mice 12 to 14 days after injection with B16 melanoma cells or B16 cells overexpressing Csf2 (B16$^{Csf2}$). Bar graphs show absolute number of colonic $T_{regs}$ in the indicated groups. All data (A to H) are shown as mean ± SD of three independent experiment with at least three mice per experiment. Student's *t* test (A to F) and one-way analysis of variance (ANOVA) Bonferroni's multiple comparison test (H and I) were performed. Statistical significance is indicated by $*P < 0.05$, $**P < 0.01$, $***P < 0.001$; ns, not significant.

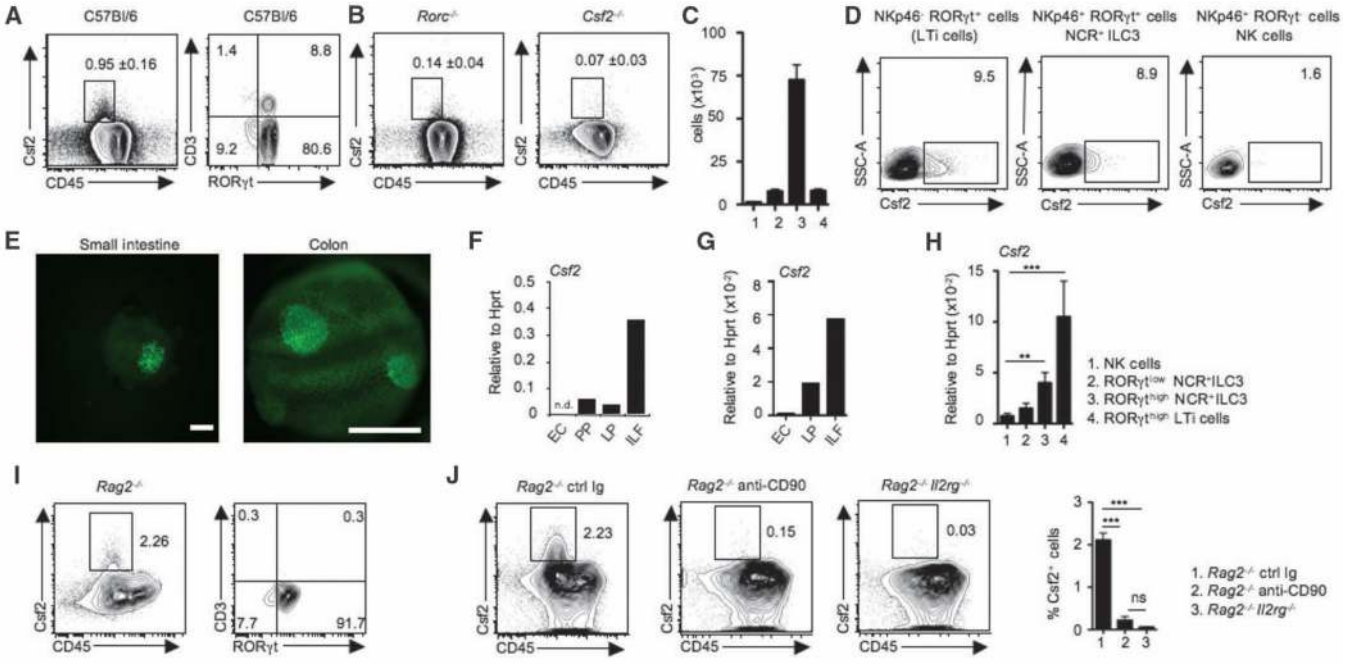


**Fig. 2. RORγt$^+$ ILCs are the major source of Csf2 in the steady-state gut**

(**A**) FACS plots show Csf2 and CD45 expression in lamina propria cells and expression of CD3 and RORγt among gated Csf2$^+$CD45$^+$ lamina propria cells (data shown are representative of 10 independent experiments including at least 5 mice per experiment). Staining was performed on ex vivo isolated cells cultured for 4 hours in the presence of Brefeldin A. (**B**) FACS plots show percentage Csf2$^+$CD45$^+$ lamina propria cells in the small intestine of *Rorc*$^{-/-}$ and *Csf2*$^{-/-}$ mice. Data are representative of at least three experiments with two mice per group and are shown as mean ± SD. (**C**) Bar graph shows absolute numbers of Csf2-producing cells in lamina propria cells. 1: Csf2$^+$CD3$^+$RORγt$^-$ T cells; 2: Csf2$^+$CD3$^+$RORγt$^+$ T cells; 3: Csf2$^+$CD3$^-$RORγt$^+$ ILCs; 4: Csf2$^+$CD3$^-$RORγt cells. (**D**) FACS plots show Csf2 expression on gated lamina propria NKp46$^-$RORγt$^+$ LTi cells, NKp46$^+$RORγt$^+$ NCR$^+$ ILC3, and NKp46$^+$RORγt$^-$ NK cells. Data are representative of six independent experiments with at least three mice per group. (**E**) Representative fluorescence stereomicroscopic photographs of live lamina propria biopsy punches obtained from *Rorc*$^{+/EGFP}$ mice. Image shows clustered enhanced green fluorescent protein (EGFP) (RORγt) expression of ILF-residing Rorc$^{+/EGFP}$ cells isolated from small intestine (left; scale bar: 100 μm) and colon (right; scale bar: 500 μm). (**F** and **G**) Quantitative reverse transcription–polymerase chain reaction (RT-PCR) analysis of *Csf2* expression in isolated intestinal epithelial cells (EC), Peyer's patches (PP), lamina propria depleted of ILFs (LP), and ILF from small intestine (F) or colon (G). Data are representative of at least two independent experiments with three mice per group. (**H**) Quantitative RT-PCR analysis of *Csf2* expression in colonic NK cells (1), RORγt$^{lo}$ NCR$^+$ ILC3 (2), RORγt$^{high}$ NCR$^+$ ILC3 (3), and RORγt$^{high}$ LTi cells (4) isolated from *Rorc*$^{+/EGFP}$ mice. (**I**) FACS plots show Csf2 and CD45 staining on total colonic lamina propria cells and expression of CD3 and RORγt among Csf2$^+$CD45$^+$ cells isolated from *Rag2*$^{-/-}$ mice (data are representative of two independent experiments with three mice per group). (**J**) FACS plots show Csf2 and CD45

staining on total colonic lamina propria cells isolated from either *Rag2*$^{-/-}$ mice, *Rag2*$^{-/-}$ mice injected with depleting anti-CD90 mAb, or *Rag2*$^{-/-}$*Il2rg*$^{-/-}$ mice. Bar graph shows percentages of Csf2$^{+}$ CD45$^{+}$ cells in each group of mice. All Csf2 staining was performed on ex vivo isolated cells cultured for 4 hours in the presence of Brefeldin A. Data are shown as mean ± SD of two independent experiments with three mice per group. One-way ANOVA Bonferroni's multiple comparison test (H and J) was performed. Statistical significance is indicated by *$P < 0.05$, **$P < 0.01$, and ***$P < 0.001$.

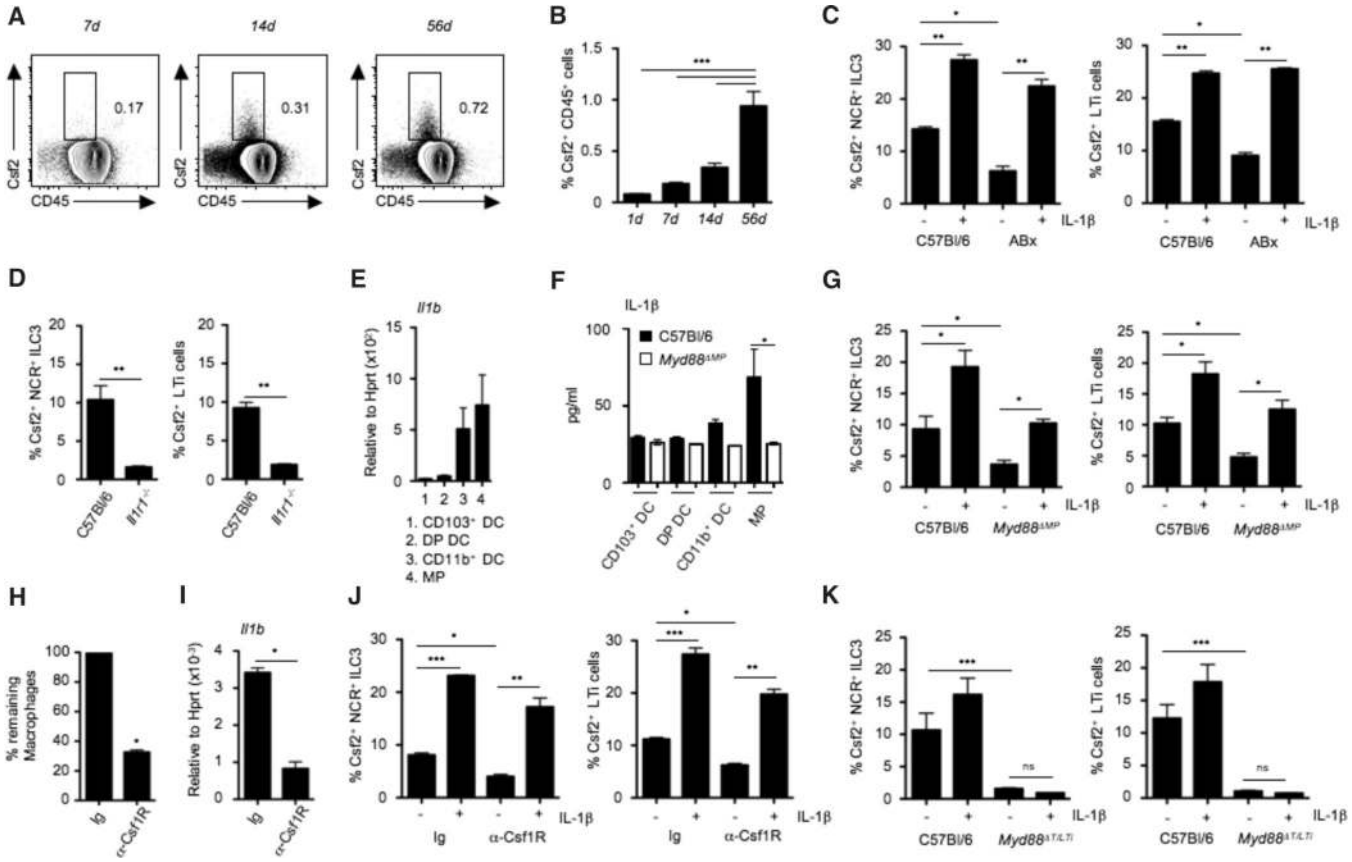


**Fig. 3. Microbiota-driven IL-1β release by intestinal macrophages regulates Csf2 production by RORγt$^+$ ILC3**

(**A**) FACS plot showing Csf2 expression in whole intestinal lamina propria CD45$^+$ cells at the indicated time points after birth. (**B**) Bar graph shows percentages of Csf2$^+$ cells among total lamina propria cells in mice at the indicated time points after birth. Data shown are the results of three independent experiments with at least three mice per group. (**C**) Percentages of Csf2$^+$ cells among gated colonic lamina propria NCR$^+$ ILC3 and LTi cells in conventional mice or mice treated with broad-spectrum antibiotics (ABx). Stains were performed on cells cultured for 4 hours with (+) or without (−) IL-1β in the presence of Brefeldin A. Data are shown as mean ± SD of three independent experiments with at least three mice per group. (**D**) Percentages of Csf2$^+$ cells among gated colonic lamina propria NCR$^+$ILC3 and LTi cells in *Il1r*$^{-/-}$ or C57Bl/6 mice. Data show the results of two independent experiments with three mice per group. (**E**) *Il1b* mRNA expression in FACS-purified colonic MNPs. Data shown are representative of two independent experiments with pooled cells of three mice. (**F**) IL-1β protein production by purified intestinal DC subsets and MPs isolated from the colonic lamina propria of C57Bl/6 and *Myd88*$^{\Delta MP}$ mice, measured by ELISA after 24 hours of culture in complete medium. Data are representative of two independent experiments with pooled cells of three mice. (**G**) Percentages of Csf2$^+$ cells among gated colonic ILC3 in *Myd88*$^{\Delta MP}$ mice. Stains were performed in cells cultured for 4 hours with or without IL-1β in the presence of Brefeldin A. Data are shown as mean ± SD of three independent experiments with at least three mice per group. (**H**) Groups of mice were injected with one injection of anti-Csf1R mAb (3 mg per mouse) or control mAb. Bar

graph shows percentages of remaining macrophages in colonic tissue. (**I**) *Il1b* expression in whole colonic tissue of mice treated with anti-Csf1R mAb or isotype control. Data are shown as mean ± SD of at least three independent experiments with three mice per group. (**J**) Percentages of $Csf2^+$ cells among gated colonic lamina propria $NCR^+$ ILC3 and LTi cells in mice treated with anti-Csf1R mAb or control mAb. Staining was performed on total cells cultured for 4 hours with or without IL-1β in the presence of Brefeldin A. Data are shown as mean ± SD of three independent experiments with three mice per group. (**K**) Csf2 production by colonic lamina propria $NCR^+$ ILC3 and LTi cells in $Myd88^{\Delta T/LTi}$ mice measured after 4 hours of culture with or without IL-1β in the presence of Brefeldin A. Data are shown as mean ± SD of three independent experiments with at least three mice per group. Student's t test (D, H, and I) or one-way ANOVA Bonferroni's multiple comparison test (B, C, F, G, J, and K) were performed. Statistical significance is indicated by $*P < 0.05$, $**P < 0.01$, and $***P < 0.001$.

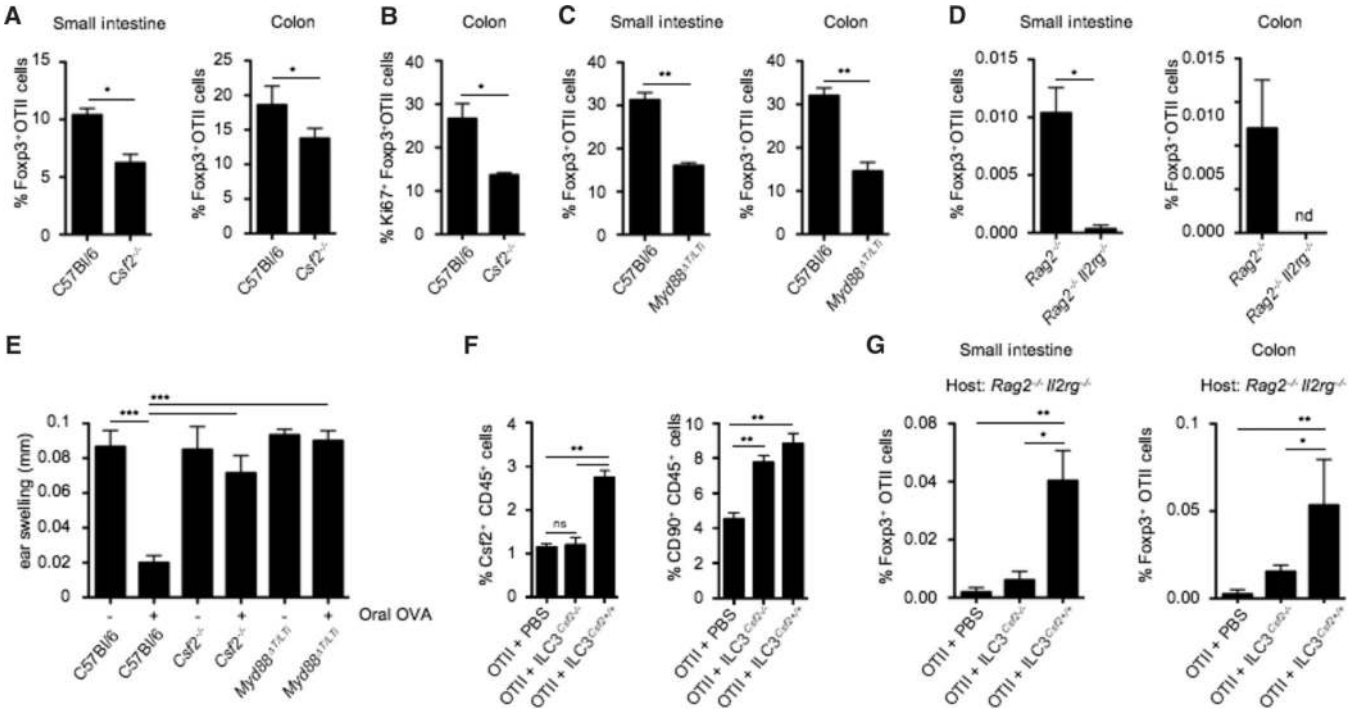


**Fig. 4. ILC3-derived Csf2 controls oral tolerance to dietary antigens**

(**A**) Naïve OTII *Rag2*$^{-/-}$ CD45.1$^{+}$ T cells were adoptively transferred into CD45.2$^{+}$ C57Bl/6 and CD45.2$^{+}$ Csf2$^{-/-}$ mice. Bar graph shows percentages of small intestinal and colonic OTII-specific Foxp3$^{+}$ $T_{regs}$ after oral feeding with OVA ad libidum. Data are shown as mean ± SD of three independent experiments with three mice per group. (**B**) Bar graph shows percentages of Ki67$^{+}$ colonic Foxp3$^{+}$ OTII T cells in C57Bl/6 and *Csf2*$^{-/-}$ mice after OVA feeding. Data are shown as mean ± SD of three independent experiments with three mice per experiment. (**C** and **D**) Naïve OTII *Rag2*$^{-/-}$ CD45.1$^{+}$ T cells were adoptively transferred into C57Bl/6 and *Myd88*$^{\Delta T/LTi}$ mice (C), or *Rag2*$^{-/-}$ and *Rag2*$^{-/-}$*Il2rg*$^{-/-}$ mice (**D**). Bar graphs show percentages of small intestinal and colonic OTII-specific Foxp3$^{+}$ $T_{regs}$ after OVA feeding. Data are shown as mean ± SD of three independent experiments with three mice per group. (**E**) *Csf2*$^{-/-}$, *Myd88*$^{\Delta T/LTi}$ and control mice were either fed (+) or not fed with OVA (–) for 7 days to induce oral tolerance. Four days later, fed mice were immunized subcutaneously with OVA (300 μg) and complete Freund's adjuvant and rechallenged 14 days later with OVA (50 μg) into the right ear, as described in the materials and methods. Skin DTH response was determined by ear swelling (mm). Data are shown as mean ± SD ($n$ = 10 mice) and are representative of two independent experiments. (**F** and **G**) Purified wild-type or *Csf2*$^{-/-}$ ILC3 were injected into *Rag2*$^{-/-}$*Il2rg*$^{-/-}$hosts, 2 weeks before injection of naïve OTII CD45.1$^{+}$ T cells. Reconstituted hosts were fed with OVA and analyzed 5 days later. (F) Bar graph shows percentages of Csf2$^{+}$ CD45$^{+}$ cells (left) and total CD90$^{+}$ CD45$^{+}$ ILCs (right) in the colonic lamina propria of the indicated host mice. Data are shown as mean ± SD of two independent experiments with three mice per group. (G) Bar graphs show percentages of small intestinal and colonic OTII-specific Foxp3$^{+}$ $T_{regs}$ after OVA feeding. Data are shown as mean ± SD of two independent experiments with three mice per group. Student's $t$ test (A to D) or one-way ANOVA Bonferroni's multiple

comparison test (E to G) were performed. Statistical significance is indicated by $*P < 0.05$, $**P < 0.01$, and $***P < 0.001$.